Predicting the properties of a new class of host-guest complexes: C60 fullerene and CB[9] cucurbituril

Journal:	*Physical Chemistry Chemical Physics*
Manuscript ID:	CP-ART-07-2014-003299.R1
Article Type:	Paper
Date Submitted by the Author:	22-Aug-2014
Complete List of Authors:	Fileti, Eudes; UNIFESP, Departamento de Ciência e Tecnologia Colherinhas, Guilherme; CEPAE, Universidade Federal de Goiás, Departamento de Física Malaspina, Thaciana; Universidade Federal de São Paulo, Departamento de Ciência e Tecnologia

Predicting the properties of a new class of host-guest complexes: C_{60} fullerene and CB[9] cucurbituril

Eudes Fileti[1], Guilherme Colherinhas[2] and Thaciana Malaspina[1]

1) Instituto de Ciência e Tecnologia, Universidade Federal de São Paulo, 12231-280, São José dos Campos, SP, Brazil.
2) Departamento de Física, CEPAE, Universidade Federal de Goiás, CP.131, 74001-970, Goiânia, GO, Brazil.

* Corresponding author. E-mail: gcolherinhas@gmail.com; thaciana.unifesp@gmail.com; fileti@gmail.com; Tel: +55 12 3309-9573; Fax: +55 12 3921-8857

TOC Graph

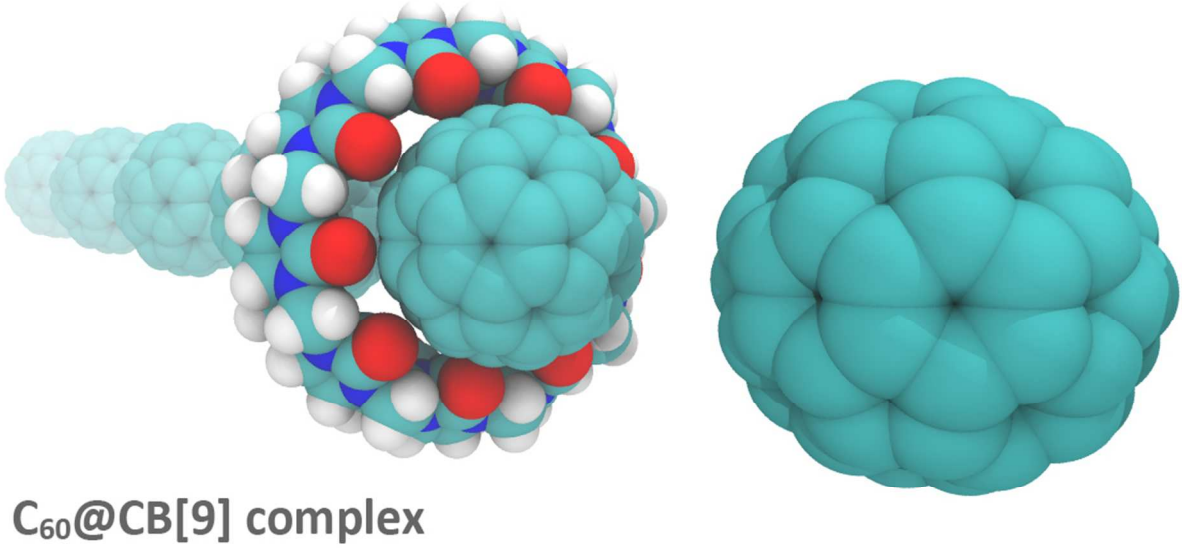

ABSTRACT

DFT, semi-empirical and classical molecular dynamics methods were used to describe the structure and stability of the inclusion complex formed by the fullerene C_{60} and the cucurbituril CB[9]. Our results indicate a high structural compatibility between the two monomers, which is evident from the potential energy curve for the inclusion process of the C_{60} into the CB[9] cavity. The interaction between the two monomers is mainly of van der Waals type and leads to a highly stable complex. Thermal contributions and environment interaction are taken into account by the free energy of binding of -224 kJ mol^{-1}, indicating that even in aqueous medium the complex remains very stable.

Keywords: *DFT, PM6, molecular dynamics, C_{60}, cucurbituril, host-guest complex*

1. Introduction

The research and development of nanomaterials in recent years has boosted several frontier research areas. [1-3] Unusual materials appear every day with innovative properties and with a wide range of possible applications. In this context, two classes of materials have attracted much attention in the last two decades. They are carbon nanostructures and macrocyclic molecular containers. The first class, which includes graphene, nanotubes and fullerenes, has been extensively studied during the last two decades. The applications of these materials range from solar cells to anti-cancer therapy.[4-16] In turn, macrocyclic nanomaterials are one of the pillars of supramolecular chemistry. Several important developments involving macrocycles such as cyclodextrins, calixarenes and, more recently, cucurbiturils have been reported recently. [17-30] The potential applications of host-guest macrocycle chemistry extend from biomedical to environmental issues.[17-23]

C_{60} and cucurbituril are outstanding representatives of each of the classes of materials mentioned above. C_{60} is a well-known nanoparticle with a wide horizon of potential applications in diverse areas, such as electronics, biomedicine, and cosmetics industry.[31, 32] For most applications, C_{60} is required to be solubilized.[7, 16, 33-35] Therefore, a strong interaction of C_{60} with a solvent is important. For example, industrial applications of light fullerenes require their fine dispersion in organic and lipophilic media, whereas biomedical applications anticipate stable aqueous phases.[32] Unfortunately, well-recognized hydrophobicity of C_{60} hinders development of such applications. The cucurbiturils, in turn, represent a family of macrocycles that possess hydrophobic hollow core and two hydrophilic ring portals (see Figure 1).[26, 30, 36, 37] These structural features are favorable for the formation of a host-guest complex. Such molecular container compounds act as

molecular receptors due to their high affinity (much higher than those of other species of macrocycles) and their high selectivity for processes that occur within its cavity. A set of promising applications such as drug delivery, molecular machines and switches, supramolecular polymers, gas purifications sensing ensembles and biomimetic systems have been presented recently.[37-39]

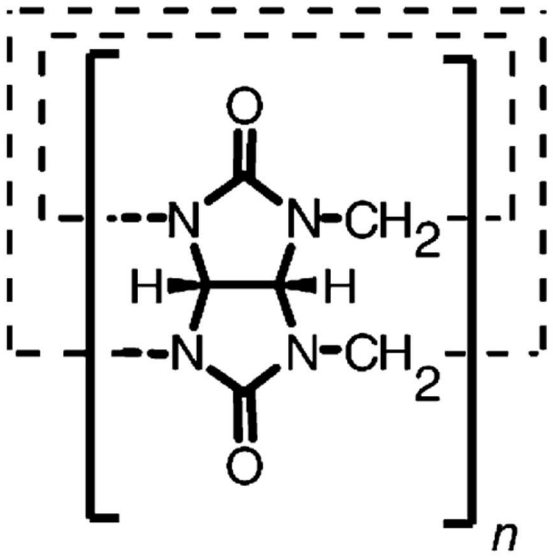

Figure 1: Cucurbit[n]uril macrocycles, CB[n].

The cucurbit[n]uril (CB[n]; n = 5, 6, 7, 8, 10) family of molecular container compounds are prepared by the condensation reaction of glycoluril and formaldehyde under strongly acidic conditions.[26, 30, 37, 39] All representatives of this family have been synthesized and well documented in literature. [26, 30, 37, 39] On the other side, cucurbiturils with $n < 5$ or $n > 10$ are not expected to be stable due to tensions between the constituent glycolurils. However, the absence of the CB[9] member is notable and curious, since the CB[10] has been obtained.[30, 40] It is important to note that CB[10] was obtained with the help of another compound, CB[5], which fits

perfectly into the CB[10] cavity reducing tension and allowing its formation in the reaction environment.[41, 42] For CB[9] a similar procedure would be necessary, however, as CB[5] does not fit into its cavity and there is no lower cucurbituril, another guest should be considered.

The C_{60} and CB[9] molecules exhibit virtually the same van der Waals radius. Furthermore, C_{60} possibly acts as an auxiliary guest in the CB[9] synthesis, the perfect fit of both nanosystems can lead to the formation of an unusual inclusion complex involving a carbon nanoparticle and a cucurbituril macrocycle. In this work, we employ density functional theory (DFT), semi-empirical hamiltonian (PM6) and atomistic-resolution molecular dynamics computations to predict structure, stability and energy of these two monomers. The CB[9] cucurbituril and its complex with fullerene C_{60} are considered for the first time.

2. Methods

2.1 Static and dynamical PM6 semi-empirical calculations

The inclusion complex involving the CB[9] cucurbituril and C_{60} fullerene, abbreviated herein as C_{60}@CB[9], consists of 222 atoms with a total of 1134 electrons. Treatment of such large systems is computationally expensive in the case of DFT or higher-level methods. Therefore, the energy-minimized structures of monomers and their complex were obtained by semi-empirical method, PM6. Although semiempirical hamiltonians may not perform perfectly for peculiar geometries, large excitations and strongly non-equilibrated systems, they account for all quantum and many-body effects. PM6 is one of the most recent parametrizations of semiempirical

methodology. The method provides an invaluable assistance in the preliminary screening of the condensed matter systems containing a significant number of electrons. A relaxed energy scan for the inclusion process of the C_{60} in the CB[9] cavity was performed. Thus it was possible to obtain reliable intermediate configurations for points between the centers of mass (R_{CM}) of each monomers separated by 0.02 nm in a range of 0.98 nm. With these relaxed structures at each point we calculate a DFT energy surface for this process, as will be discussed in the next section. To access possible conformational changes in the CB[9], nuclear trajectory calculations were performed in vacuum at the PM6 level by using the atom-centered density matrix propagation (ADMP) molecular dynamics technique.[43] Time-step of 0.1 fs was used during the NVE simulations. In total, 5000 time-steps were performed in the case of a single molecule of cucurbituril. The fictitious electron mass was set to 0.1 a.m.u. and initial kinetic energy was set to the system to represent its temperature at 300K. All the ADMP calculations were started from the corresponding PM6 optimized geometries.

2.2 DFT calculations

The complexation energy and the surface energy for the inclusion of C_{60} in cucurbituril were determined using the optimized structures. These structures were optimized using PM6.[44] For each structure (monomers, complex and intermediaries), energies were described by using the recently proposed high-quality hybrid exchange-correlation functional, ωB97X-D.[45] The exchange energy was combined with the exact energy from the Hartree-Fock theory. Empirical atom-atom dispersion correction was included. According to Chai and Head-Gordon,[45] the ωB97X-D functional simultaneously yields an improved accuracy for thermochemistry, electron

kinetics, and non-covalent interactions and therefore must describe satisfactorily the hydrophobic character of the interaction between the monomers under investigation. We construct the wave function using 6-31G(d,p) basis set that for this system was composed of 5082 primitive gaussian functions. From these calculations we also obtained the set of partial electrostatic charges for the CB[9] monomer. These partial charges were determined within ChelpG scheme[46] and used in molecular interaction potential for molecular dynamics simulations, as discussed in the subsequent section. All semi-empirical and DFT calculations were performed using the Gaussian 09 program.[47]

2.3 Molecular dynamics simulations

We use the optimized structures as a reference for our intra and intermolecular interaction model. This model excellently captures all interactions between the monomers and was based on the CHARMM36 force field.[48, 49] The intermolecular interaction model used to describe the C_{60} molecule was parameterized and validated in the previous studies.[34, 35, 50-52] For CB[9] all Lennard-Jones parameters were extracted from the CHARMM36 force field while partial charges were taken from ChelpG procedure employing DFT calculations mentioned above. The force constants for the intramolecular degrees of freedom were adjusted to reproduce the rigidity of macrocycles as it ascertained by semi-empirical molecular dynamics. Simulations in vacuum and water were conducted to allow obtaining the difference in free energy associated with the thermodynamic cycle shown in Figure 2. Details of these simulations are presented in the supporting material. The elucidation of free energy differences due to changes in molecular interactions is used here to estimate the binding free energy for the complexation of C_{60} and CB[9]. Free energy changes were calculated using the stochastic molecular dynamics associated

with thermodynamic integration scheme[53] by gradually decoupling a solute molecule from the solvent using the identity:[54]

$$\Delta G = \int_{\lambda=0}^{\lambda=1} \langle \frac{dH(\lambda)}{d\lambda} \rangle \, d\lambda$$

where *H* is the parametrized Hamiltonian, for which the coupled state ($\lambda = 1$) corresponds to a simulation with C_{60} fully interacting with the medium (solvent and host CB[9]) and the uncoupled state ($\lambda = 0$) corresponds to a simulation considering the solute without interaction with the medium. To avoid singularities, we have used the soft-core interactions for the LJ interactions.[55-57] For each process shown at the thermodynamic cycle, 26 values for λ were used, from 0 to 1 to calculate the change free energy. For all simulations a non-uniform Δλ set was employed: from 0.00 to 0.20 at intervals of 0.02 and from 0.24 to 1.00 at intervals of 0.04. For each simulation, the system was equilibrated for 1 ns followed by 10 ns run. The binding free energy was then obtained by energetic balance of the thermodynamic cycle showed at Figure 2. All stochastic molecular dynamics simulations have been performed with the GROMACS 4.6 program.[56, 57]

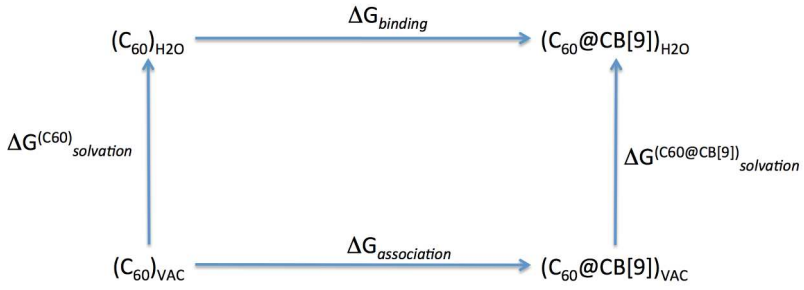

Figure 2: Thermodynamic cycle used to determine the biding free energy of the fullerene C_{60} and cucurbituril CB[9].

3. Results and Discussions

The vacuum equilibrium structure to each member of the CB[n] homologous series of n varying from 5 to 12 was determined previously.[58] In condensed medium strain forces lead to flattening of the ring when a critical size n is achieved (this supposedly occurs for n > 8), but in vacuum all members keep their perfectly circular cavity. The cavity diameter of these cucurbiturils grows linearly with n, going 0.39 nm for CB[5] up to 1.5 nm for CB[12]. The diameter of cucurbituril CB[9] is expected to be 1.0 nm in vacuum.[58] For C_{60}, the approximate geometrical diameter is about 0.70 nm.[59] Therefore, considering the van der Waals radii of these two monomers it was found that C_{60} fits perfectly into the cavity of CB[9]. Figure 3 shows the relative size of these molecules and the inclusion complex formed by them.

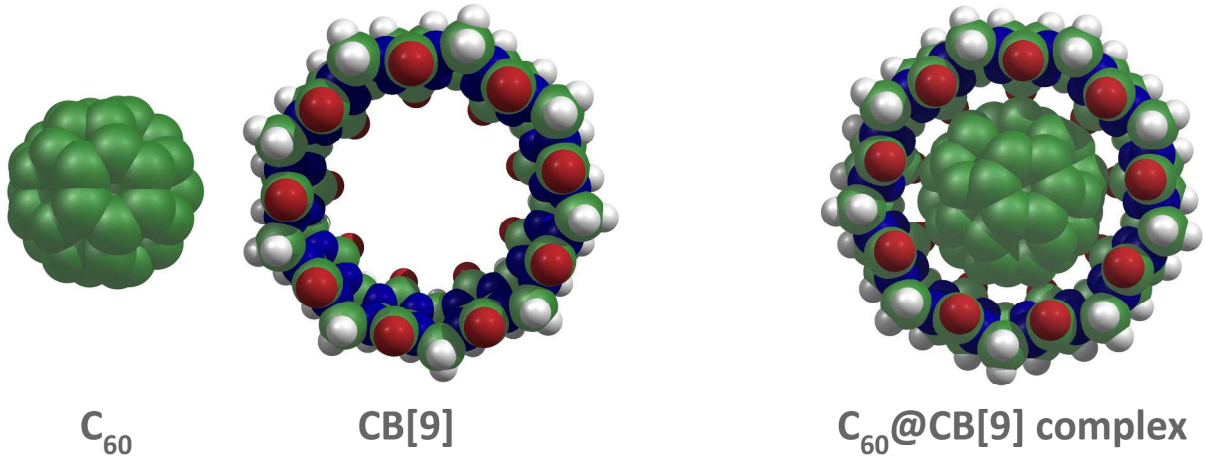

Figure 3: Molecular representation for C_{60} and CB[9] monomers and C_{60}@CB[9] complex in scale.

The main indicator for the stability of the complex is the binding energy of C_{60} and CB[9]. The binding energy of the C_{60}@CB[9] resulting complex was obtained from the energy difference between the energy of the complex and of the isolated monomers defined as follows:

$$E_{binding} = E_{C_{60}@\mathrm{CB[9]}} - E_{CB[09]} - E_{C_{60}}$$

The obtained binding energy is -350 kJ mol^{-1} and indicates that complexation in vacuum is highly favorable. To get an idea of the magnitude of this energy we can compare it with the stability of other host-guest complexes involving the most studied cucurbiturils, CB[7]. For example, the binding energy between cucurbituril CB[7] is about -118 kJ mol^{-1}, when bounded to cisplatin, [60] -41 kJ mol^{-1}, when bounded to cyclohexylammonium ion,[61] -54 kJ mol^{-1}, when bounded to di-*tert*-butyl nitroxide,[62] and -189 kJ mol^{-1} when bounded to dimethyl-pyrilium cation.[63] Of course we can not say that the C_{60}@CB[9] is much more stable than these mentioned, since C_{60} is much large guests but is important to note that this complex is actually quite stable even being stabilized by van der Waals forces.

The process of inclusion of C_{60} into the CB[9] was scanned gradually through ωB97X-D/6-31G(d,p) single point calculations on PM6 optimized intermediates. Figure 4 shows the potential energy curve and indicates, as expected, that the stability of the complex is achieved when the C_{60} reaches the center of the CB[9] cavity, wherein the energy of complexation is largest, ~246 kJ mol^{-1}. The zoomed graph (right of Figure 4) shows that before reaching the center of the cavity, fullerene passes through an intermediate minimum of -64 kJ mol^{-1}, at 0.62 nm. A barrier of 40.0 kJ mol^{-1} from this local minimum, at 0.34 nm separate it from the global minimum. This barrier is below the level of dissociation of the complex and is comparable to kT, therefore the

process of inclusion is expected to occur under normal conditions. This profile demonstrates the high affinity of the C_{60} and cucurbituril CB[9] that results from the strong non-covalent collective interactions between the hydrophobic CB[9] internal cavity and the outer C_{60} surface. This strong interaction is favored not only from the standpoint of energy but also the geometrical point of view since the cucurbituril cavity is concave while the C_{60} surface is convex which favors an almost perfect fit. Energy surface already reflects this fact.

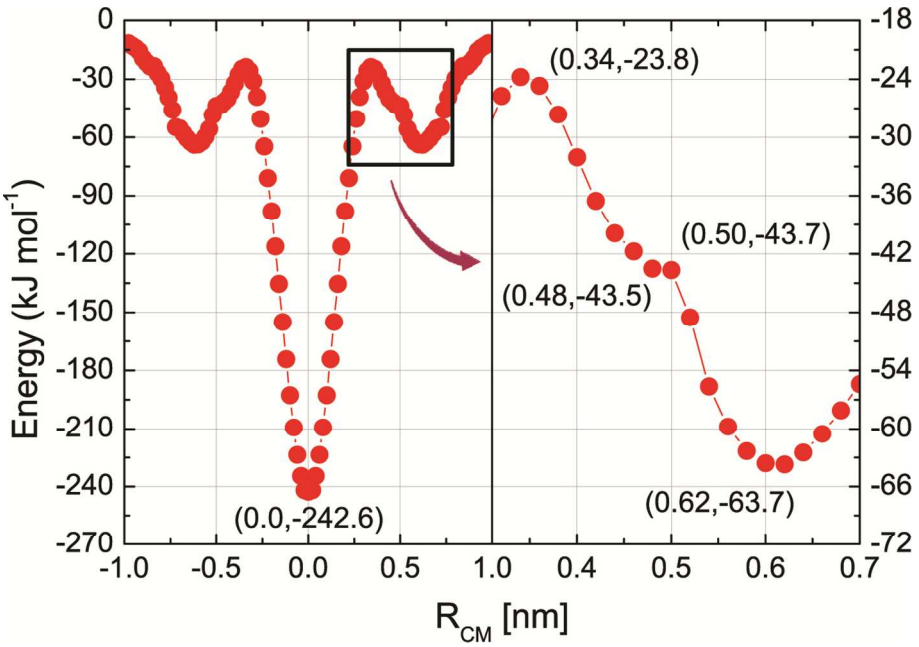

Figure 4: ωB97X-D/6-31G(d,p) potential energy scan over PM6 optimized structures for the inclusion complex C_{60}@CB[9], while the guest fullerene passing through the cucurbituril cavity along the host symmetric axis. The sum of energies of isolated CB[9] and C_{60} was taken as reference at the zero of energy axis. The profile is corrected against BSSE.

The approach of the C_{60} to the hydrophilic CB[9] portal induces profound changes in the electron cloud of the fullerene. The ωB97X-D/6-31G(d,p) results for the Mulliken atomic charges shows that there is charge transfer between the monomers during the inclusion process. From the Figure S5 (supporting information), it can be seen that for the minimum energy configuration (R_{CM} = 0 nm) the charges on monomers are about +0.062 *e* and -0.062 *e* for CB[9] and C_{60} respectively. During the inclusion process we can observe the maximum charge redistribution of + 0.109 *e* and -0.109 *e* to C_{60} and CB[9] monomeric species, respectively. This effect contributes to the observed maximum for the complex dipole moment that occurs at center-of-mass distance of 0.48 nm. This charge transfer is inherently associated to a large variation in the dipole moment of the complex during inclusion. Figure 5, which shows the dipole moment induced in the complex as the inclusion process develops. Both C_{60} and CB[9] in vacuum are nonpolar molecules. Furthermore, the complex itself also displays just a residual dipole moment. However, it may be seen that near the site of contact the induced dipole moment reaches high values, reaching 6.7 D when the separation from the center of mass is 0.48 nm. In Figure 5 we present a molecular representation indicating the dipole moment direction for the mentioned situation.

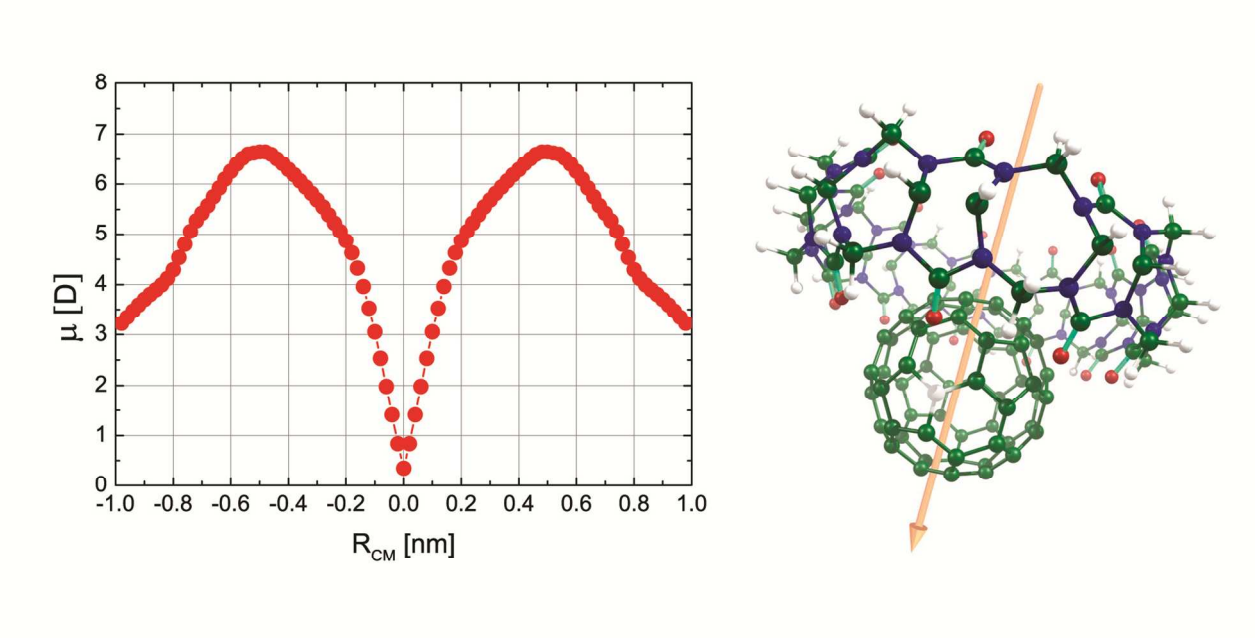

Figure 5: Variation of the induced dipole moment (D) calculated as a function of separation distance between the centers of mass of the molecules. At right, the maximum-dipole molecular structure indicating the direction of the induced dipole moment.

The resulting structure formed in vacuum by inclusion of fullerene into cucurbituril is highly stable and only very intense disturbances would cause its separation. However this stability can be reduced when heat effect or environment interactions are taken into account. For an analysis of the thermodynamics of this system we performed classical molecular dynamics simulations to determine the binding free energy in aqueous media. Before that we conducted a semi-empirical molecular dynamic study of the CB[9] molecule in vacuum aiming confirm its structural stability and also obtain reliable intramolecular parameters for fitting our classic model.

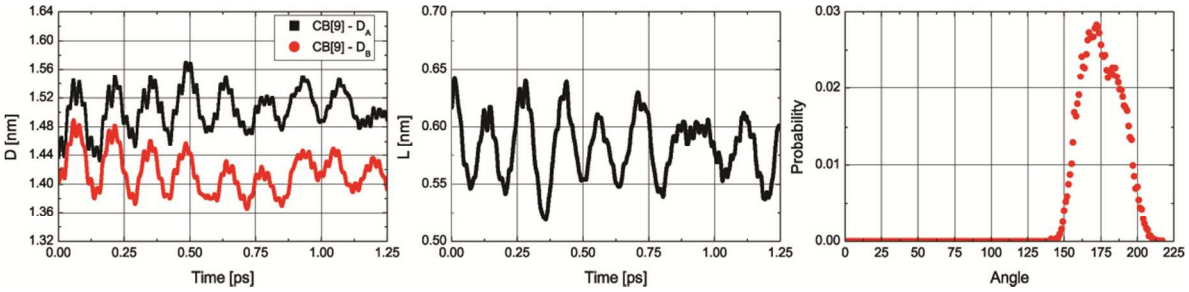

Figure 6: CB[9] intramolecular parameters from PM6 ADMP molecular dynamics. At left larger and lower diameters (in nm), at middle the height (in nm) and at right the distribution of angles for the dihedral N-O-C-N (in degrees).

Figure 6 shows three different structural parameters of the CB[9] obtained from the PM6 molecular dynamics. The first refers to the height of the cucurbituril, which was measured as the distance between the planes of oxygen atoms of the rings. This height varies with appreciable stretching (about 5%) around the mean value of 0.58 nm. The second is the diameter calculated for two selected opposite carbons pair, representing the largest (1.50±0.03 nm) and the smallest (1.41±0.03 nm) average value found for this parameter. This indicates that gas-phase CB[9] must show a slightly elongated shape. Finally, the N-O-C-N dihedral angle that measure the mobility of the C=O bond and which are related to the opening of the cucurbituril portals are also presented. The average value for this angle is 172.6^{o} with a standard deviation of 19^{o}, which indicates relatively small amplitude of oscillation to open the gate. Overall, semi-empirical molecular dynamics shows a relatively stiff structure for the macrocycle and despite structural changes its structure keeps the main characteristics of the optimized macrocycle.

The interaction molecular model for the CB[9] molecule was based on the parameters of the CHARMM36 force field with partial charges obtained by *ab initio* calculations. A additional adjustment was made in the spring constants of the angles and dihedral to take into account the relative stiffness of the CB[9] macrocycle. Vacuum simulations reproduced satisfactorily these intramolecular parameters. With this potential we performed all simulations required by the thermodynamic cycle from Figure 2 and allow us determine the binding free energy in aqueous media. We emphasize here that in our model only van der Waals interactions are considered for C_{60}, so that all the energy that stabilizes the complex is derived only from the Lennard-Jones part of the interaction potential. This aspect is interesting because as the C_{60} is neutral and uncharged species and its complexation with cucurbituril eliminates all contributions from charge-dipole interactions that are almost always present in this type of systems and that dominate the host-guest interaction. Furthermore, as the fullerene is uncharged, all of the electrostatic site interactions between the monomers are eliminated. That way one can rationalize the fullerene/cucurbituril complexation process only in terms of hydrophobic interactions. The absolute binding free energy in water, in turn, is -224 kJ mol^{-1} indicating that interactions with liquid water reduces the stability of the complex by 63 kJ mol^{-1}. For contextualizing the magnitude of these values we observed first that, the binding constants for neutral guests with cucurbituril hosts are typically orders of magnitude lower than the corresponding for charged guests. For example, the affinity constant of a di-cationic adamantane with cucurbituril CB[6] is 5.5×10^{15} (equivalent to a free binding energy of 88 kJ mol^{-1}) while the constant for a neutral adamantane derivative host is 2.3×10^{10} (equivalent to a free binding energy of 60.0 kJ mol^{-1}).[64] The binding energy of 88 kJ mol^{-1} for a di-cationic guest has been considered as one of the largest binding energies ever found for host-guest systems.[26, 64] In this context, the apolar-neutral-

guest C_{60}@CB[9] complex present a relatively high binding energy and indicates that non-additive C_{60}/CB[9] attraction resulting in a stable van der Waals complex and represents a new class of host-guest systems.

4. Conclusions

In this work we use DFT, semi-empirical and classical molecular dynamics methods to describe the structure and stability of the inclusion complex formed by the fullerene C_{60} and the cucurbituril CB[9]. Our results indicate a high structural compatibility between the two monomers, which is evident from the potential energy curve for the inclusion process of the C_{60} into the CB[9] cavity. The interaction between the two monomers is mainly of van der Waals type and leads to a highly stable complex. Thermal contributions and environment interaction are taken into account by the free energy of binding of -224 kJ mol^{-1}, indicating that even in aqueous medium the complex remains very stable.

It is known that cucurbiturils with odd n (CB[5] and CB[7]) are water-soluble, while those with even n (CB[6], CB[8] and CB[10]) are not.[26, 38] The reasons for this are not well understood, but we can assume that the CB[9] will be soluble in water. Furthermore, it has been revealed that the family of cucurbituril has low or none toxicity.[38] In this sense the complexation between C_{60} and CB[9] can dramatically reduce the main problems related to biomedical applications of fullerene: toxicity and very low water-solubility. This work therefore may be useful for future experimental investigations aimed to synthesize, characterize and apply host-guest complexes involving fullerenes and cucurbiturils species.

5. Supporting Information

Further technical aspects and structural analysis are also provided. This material is available free of charge via the Internet at http://pubs.acs.org.

6. Acknowledgments

This work was supported by grants from Brazilian agencies FAPESP and CNPq. The authors thank Paulo Burke for technical support and Dr. Vitaly Chaban for his critical review.

7. References

1. D. Li and Y. N. Xia, *Nat Mater*, 2004, 3, 753-754.
2. A. D. Kelkar, D. J. C. Herr and J. G. Ryan, eds., *Nanoscience and Nanoengineering: Advances and Applications* CRC Press, New York, 2014.
3. H. J. Fecht and K. Brühne, eds., *Carbon-based Nanomaterials and Hybrids: Synthesis, Properties, and Commercial Applications (Critical Concepts in Historical Studies)*, 2014.
4. P. Salice, E. Fabris, C. Sartorio, D. Fenaroli, V. Figà, M. P. Casaletto, S. Cataldo, B. Pignataro and E. Menna, *Carbon*, 2014, 74, 73-82.
5. O. V. Penkov, V. E. Pukha, A. Y. Devizenko, H. J. Kim and D. E. Kim, *Nano Lett*, 2014, 14, 2536-2540.
6. M. Calvaresi, F. Arnesano, S. Bonacchi, A. Bottoni, V. Calo, S. Conte, G. Falini, S. Fermani, M. Losacco, M. Montalti, G. Natile, L. Prodi, F. Sparla and F. Zerbetto, *ACS Nano*, 2014, 8, 1871-1877.
7. E. E. Fileti and V. V. Chaban, *The Journal of Physical Chemistry Letters*, 2014, DOI: 10.1021/jz500609x, 1795-1800.
8. M. F. De Volder, S. H. Tawfick, R. H. Baughman and A. J. Hart, *Science*, 2013, 339, 535-539.
9. A. Bianco, H.-M. Cheng, T. Enoki, Y. Gogotsi, R. H. Hurt, N. Koratkar, T. Kyotani, M. Monthioux, C. R. Park, J. M. D. Tascon and J. Zhang, *Carbon*, 2013, 65, 1-6.
10. E. Miyako, T. Sugino, T. Okazaki, A. Bianco, M. Yudasaka and S. Iijima, *ACS Nano*, 2013, 7, 8736-8742.
11. F. Cataldo, O. Ursini and G. Angelini, *Carbon*, 2013, 62, 413-421.
12. A. Aldinucci, A. Turco, T. Biagioli, F. M. Toma, D. Bani, D. Guasti, C. Manuelli, L. Rizzetto, D. Cavalieri, L. Massacesi, T. Mello, D. Scaini, A. Bianco, L. Ballerini, M. Prato and C. Ballerini, *Nano Lett*, 2013, 13, 6098-6105.
13. M. F. Serag, K. Braeckmans, S. Habuchi, N. Kaji, A. Bianco and Y. Baba, *Nano Lett*, 2012, 12, 6145-6151.
14. R. Leary and A. Westwood, *Carbon*, 2011, 49, 741-772.
15. X. Zhang, J. Yin, C. Peng, W. Hu, Z. Zhu, W. Li, C. Fan and Q. Huang, *Carbon*, 2011, 49, 986-995.
16. G. Colherinhas, T. L. Fonseca and E. E. Fileti, *Carbon*, 2011, 49, 187-192.

17. Y. Jin, Q. Wang, P. Taynton and W. Zhang, *Acc Chem Res*, 2014, 47, 1575-1586.
18. A. de Juan, Y. Pouillon, L. Ruiz-Gonzalez, A. Torres-Pardo, S. Casado, N. Martin, A. Rubio and E. M. Perez, *Angew Chem Int Ed Engl*, 2014, 53, 5394-5400.
19. G. Parvari, S. Annamalai, I. Borovoi, H. Chechik, M. Botoshansky, D. Pappo and E. Keinan, *Chem Commun (Camb)*, 2014, 50, 2494-2497.
20. M. Wang, C. Wang, X. Q. Hao, J. Liu, X. Li, C. Xu, A. Lopez, L. Sun, M. P. Song, H. B. Yang and X. Li, *J Am Chem Soc*, 2014, 136, 6664-6671.
21. G. Ohlendorf, C. W. Mahler, S. S. Jester, G. Schnakenburg, S. Grimme and S. Hoger, *Angew Chem Int Ed Engl*, 2013, 52, 12086-12090.
22. Y. Kim, W. Li, S. Shin and M. Lee, *Acc Chem Res*, 2013, 46, 2888-2897.
23. Y. Zhao, H. K. Cho, L. Widanapathirana and S. Y. Zhang, *Accounts of Chemical Research*, 2013, 46, 2763-2772.
24. A. Martinez, C. Ortiz Mellet and J. M. Garcia Fernandez, *Chem Soc Rev*, 2013, 42, 4746-4773.
25. M. Xue, Y. Yang, X. Chi, Z. Zhang and F. Huang, *Acc Chem Res*, 2012, 45, 1294-1308.
26. E. Masson, X. Ling, R. Joseph, L. Kyeremeh-Mensah and X. Lu, *RSC Advances*, 2012, 2, 1213.
27. M. X. Wang, *Acc Chem Res*, 2012, 45, 182-195.
28. F. Biedermann, V. D. Uzunova, O. A. Scherman, W. M. Nau and A. De Simone, *J Am Chem Soc*, 2012, 134, 15318-15323.
29. Z. Huang, S. K. Kang, M. Banno, T. Yamaguchi, D. Lee, C. Seok, E. Yashima and M. Lee, *Science*, 2012, 337, 1521-1526.
30. J. Lagona, P. Mukhopadhyay, S. Chakrabarti and L. Isaacs, *Angew Chem Int Ed Engl*, 2005, 44, 4844-4870.
31. E. Sheka, ed., *Fullerenes: Nanochemistry, Nanomagnetism, Nanomedicine, Nanophotonics*, CRC Press, New York, 2011.
32. R. Bakry, R. M. Vallant, M. Najam-ul-Haq, M. Rainer, Z. Szabo, C. W. Huck and G. K. Bonn, *Int J Nanomedicine*, 2007, 2, 639-649.
33. C. Maciel and E. E. Fileti, *Chemical Physics Letters*, 2013, 568-569, 75-79.
34. V. V. Chaban, C. Maciel and E. E. Fileti, *The Journal of Physical Chemistry B*, 2014, 118, 3378-3384.
35. V. V. Chaban, C. Maciel and E. E. Fileti, *Journal of Solution Chemistry*, 2014, DOI: 10.1007/s10953-014-0155-6.
36. H. Yang, B. Yuan, X. Zhang and O. Scherman, *Accounts of chemical research*, 2014, DOI: 10.1021/ar500105t.
37. L. Isaacs, *Accounts of chemical research*, 2014, DOI: 10.1021/ar500075g.
38. G. Hettiarachchi, D. Nguyen, J. Wu, D. Lucas, D. Ma, L. Isaacs and V. Briken, *PloS one*, 2010, 5.
39. X. Ma and H. Tian, *Accounts of chemical research*, 2014, DOI: 10.1021/ar500033n.
40. D. Lucas, T. Minami, G. Iannuzzi, L. Cao, J. Wittenberg, P. Anzenbacher and L. Isaacs, *Journal of the American Chemical Society*, 2011, 133, 17966-17976.
41. I. D. Anthony, J. B. Rodney, P. A. Alan, L. Susan, R. L. Gareth and D. Ian, *Angewandte Chemie International Edition*, 2002, 41.
42. I. Lyle, *Chemical Communications*, 2009, DOI: 10.1039/b814897j.
43. H. B. Schlegel, S. S. Iyengar, X. Li, J. M. Millam, G. A. Voth, G. E. Scuseria and M. J. Frisch, *The Journal of Chemical Physics*, 2002, 117, 8694.
44. J. J. Stewart, *Journal of molecular modeling*, 2007, 13, 1173-1213.
45. J. D. Chai and M. Head-Gordon, *J Chem Phys*, 2009, 131, 174105.
46. C. M. Breneman and K. B. Wiberg, *Journal Of Computational Chemistry*, 1990, 11.
47. M. J. Frish and e. al., Gaussian, Inc., Wallingford CT, 2009.

48. R. B. Best, X. Zhu, J. Shim, P. E. Lopes, J. Mittal, M. Feig and A. D. Mackerell, Jr., *J Chem Theory Comput*, 2012, 8, 3257-3273.
49. E. Hatcher, O. Guvench and A. D. Mackerell, Jr., *J Chem Theory Comput*, 2009, 5, 1315-1327.
50. C. Maciel, E. E. Fileti and R. Rivelino, *J. Phys. Chem. B, 2009, 113 (20)*, 2009, 113, 7045–7048.
51. G. Colherinhas, T. L. Fonseca and E. E. Fileti, *Carbon*, 2011, 49, 187.
52. T. Malaspina, E. E. Fileti and R. Rivelino, *Journal of Physical Chemistry B*, 2007, 111, 11935-11939.
53. A. Leach, *Molecular Modelling: Principles and applications*, Prentice Hall, New York, 2001.
54. M. R. Shirts, J. W. Pitera, W. C. Swope and V. S. Pande, *J. Chem. Phys.* , 2003, 119, 5740.
55. T. C. Beutler, A. E. Mark, R. C. van Schaik, P. R. Greber and W. F. van Gunsteren, *Chem. Phys. Lett.*, 1994, 222.
56. E. Lindahl, B. Hess and D. van der Spoel, *Journal of Molecular Modeling*, 2001, 7, 306-317.
57. H. J. C. Berendsen, D. van der Spoel and R. van Drunen, *Computer Physics Communication*, 1995, 91, 43-56.
58. V. Gobre, R. Pinjari and S. Gejji, *The journal of physical chemistry. A*, 2010, 114, 4464-4470.
59. G. B. Adams, M. O'Keeffe and R. S. Ruoff, *The Journal of Physical Chemistry*, 1994, 98, 9465-9469.
60. N. Zabiollah Bolboli, Y. Faezeh and B. Sara, *Journal of Molecular Liquids*, 2012, 166.
61. Y. Ji-Sheng, W. Fu-Gen, T. Le-Fu, L. Jun-Jie and Y. Zhi-Wu, *Physical Chemistry Chemical Physics*, 2011, 13.
62. S. Mariana, S. Shulamith and A. V. Frederick, *The Journal of Physical Chemistry A*, 2012, 116.
63. A. Thangavel, C. Sotiriou-Leventis, R. Dawes and N. Leventis, *The Journal of organic chemistry*, 2012, 77, 2263-2271.
64. S. Moghaddam, C. Yang, M. Rekharsky, Y. H. Ko, K. Kim, Y. Inoue and M. K. Gilson, *J Am Chem Soc*, 2011, 133, 3570-3581.